Dynamic NMR Investigation of the Cope Rearrangement in Solutions of Monosubstituted Bullvalenes

R. Poupko,[†] H. Zimmermann,[‡] K. Müller,[§] and Z. Luz*,[†]

Contribution from The Weizmann Institute of Science, 76100 Rehovot, Israel, Max-Planck-Institut für Medizinische Forschung, AG Molekülkristalle, D-69120 Heidelberg, Germany, and Institut für Physikalische Chemie, Universität Stuttgart, D-7000 Stuttgart 80, Germany

Received November 28, 1995. Revised Manuscript Received May 14, 1996[⊗]

Abstract: High resolution carbon-13, fluorine-19, and proton NMR measurements in solutions of the monosubstituted bullvalenes, $C_{10}H_9X$ with X = F, CN, and COOH, as function of temperature are reported. The spectra at low temperatures exhibit signals due to more than one isomer (three for X = F and two for X = CN, COOH). On heating the peaks broaden due to bond shift (Cope) rearrangement involving the various isomers. Detailed analysis of the line shapes shows that in all cases interconversion between the four possible isomers must be assumed, even though the concentration of some of them is too weak to be observed. For fluorobullvalene a complete analysis of the interconversion kinetics and equilibria is presented. For cyanobullvalene and bullvalenecarboxylic acid only a semiquantitative analysis of the results was made.

Introduction

The study of the degenerate Cope rearrangement in bullvalene and bullvalene derivatives in solution was the subject of numerous studies in particular in the 1960s and 1970s.[1−7] Particularly useful for these studies has been high resolution NMR of ^1H and ^{13}C, which provided information on the equilibria and interconversion kinetics between the different isomers. These studies also promoted much work on the relation between chemical rearrangement processes and Graph Theory.[8] More recently it was found by carbon-13 and deuterium NMR that bullvalene also undergoes Cope rearrangement in the solid phase.[9−13] For the rearrangement reaction to preserve the crystal order the process, in this case, must be coupled with an appropriate reorientation that restores the molecules to their original orientation in the lattice. When one considers substituted bullvalenes the problem becomes more complicated. In solution usually several interconverting isomers coexist, and the rearrangement process becomes correspondingly more complex, involving a number of independent rate constants. Such complex dynamic schemes were considered by the earlier workers,[3−7] but a detailed quantitative analysis was so far not carried out. In the solid state several situations may be envisioned. For example the crystals may be ordered, consisting of only one[7] or of a stoichiometric mixture of several isomers. Alternatively the crystal may contain one or several isomers but in an orientationally disordered state and not necessarily in a stoichiometric ratio. It may seem that Cope rearrangement of substituted bullvalenes in ordered crystals will be strongly hindered by the requirement that the orientation of the substituent must be fixed in the crystal, while in disordered crystals rearrangement may be fast and coupled with rapid molecular reorientation. So far no dynamic studies on substituted bullvalenes in the solid state were carried out, and in fact very little is known on the crystal structure of such compounds. An exception is ref 7 where it is shown that ethylthiobullvalene crystallizes as a single isomer.

In this series of papers we consider the Cope rearrangement dynamics of a number of monosubstituted bullvalenes in solution and in the solid state. The present paper deals specifically with solutions of the three such bullvalenes, with X = F, CN, and COOH. We present detailed dynamic measurements on solutions of these compounds using predominantly carbon-13 and fluorine-19 NMR. In two companion papers[14,15] we report on dynamic studies of these compounds in the solid state.

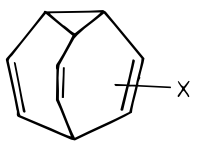

The general scheme for the Cope rearrangement in bullvalene and monosubstituted bullvalenes was discussed by several earlier workers.[1−7] Monosubstituted bullvalenes can exist as four

[†] The Weizmann Institute of Science.
[‡] Max-Planck-Institut für Medizinische Forschung.
[§] Universität Stuttgart.
[⊗] Abstract published in *Advance ACS Abstracts,* August 1, 1996.

(1) Schröder, G.; Oth, J. F. M. *Angew. Chem.* **1967**, *458*, 79.
(2) Oth, J. F. M.; Müllen, K.; Gilles, J.-M.; Schröder, G. *Helv. Chim. Acta* **1974**, *57*, 1415.
(3) Oth, J. F. M.; Merenyi, R.; Röttele, H.; Schröder, G. *Tetrahedron Lett.* **1968**, 3941.
(4) Oth, J. F. M.; Merenyi, R.; Nielsen, J.; Schröder, G. *Chem. Ber.* **1965**, *98*, 3385.
(5) Hoogzand, C.; Nielsen, J.; Oth, J. F. M. *Tetrahedron Lett.* **1970**, 2287.
(6) Oth, J. F. M.; Machens, H.; Röttele; Schröder, G. *Annalen (Liebigs Ann. Chem. Bd.)* **1971**, *745*, 112.
(7) Luger, P.; Roth, K. *J. Chem. Soc., Perkin Trans. II* **1989**, 649.
(8) For a recent paper, see: Brocas, J. *J. Math. Chem.* **1994**, *15*, 389. See, also: Ugi, I.; Dugundji, J.; Kopp, R.; Marquarding, D. In Lecture Notes in Chemistry; Berthier, G., Dewar, M. J. S., Fischer, H., Fukui, K., Hall, G. G., Hartmann, H., Hinze, J., Jaffe, H. H., Jortner, J., Kutzelnigg, W., Ruedenberg, K., Scrocco, E., Eds.; Springer-Verlag, Berlin, 1984; Vol. 36, p 141. Chemical Applications of Graph Theory; Balaban, A. T., Ed.; Academic Pres: London, 1976. Gimarc, B. M.; Brant, A. R. *J. Chem. Inf. Comput. Sci.* **1994**, *34*, 1167.
(9) Meier, B. H.; Earl, W. L. *J. Am. Chem. Soc.* **1985**, *107*, 5553.
(10) Schlick, S.; Luz, Z.; Poupko, R.; Zimmermann, H. *J. Am. Chem. Soc.* **1992**, *114*, 4315.
(11) Titmann, J. J.; Luz, Z.; Spiess, H. W. *J. Am. Chem. Soc.* **1992**, *114*, 3765.
(12) Luz, Z.; Poupko, R.; Alexander, S. *J. Chem. Phys.* **1993**, *99*, 7544.
(13) Müller, A.; Haeberlen, U.; Zimmermann, H.; Poupko, R.; Luz, Z. *Molec. Phys.* **1994**, *81*, 1239.
(14) Müller, K.; Zimmermann, H.; Krieger, C.; Poupko, R.; Luz, Z. *J. Am. Chem. Soc.* **1996**, *118*, 8006.
(15) Poupko, R.; Müller, K.; Krieger, C.; Zimmermann, H.; Luz, Z. *J. Am. Chem. Soc.* **1996**, *118*, 8015.

S0002-7863(95)04004-2 CCC: $12.00

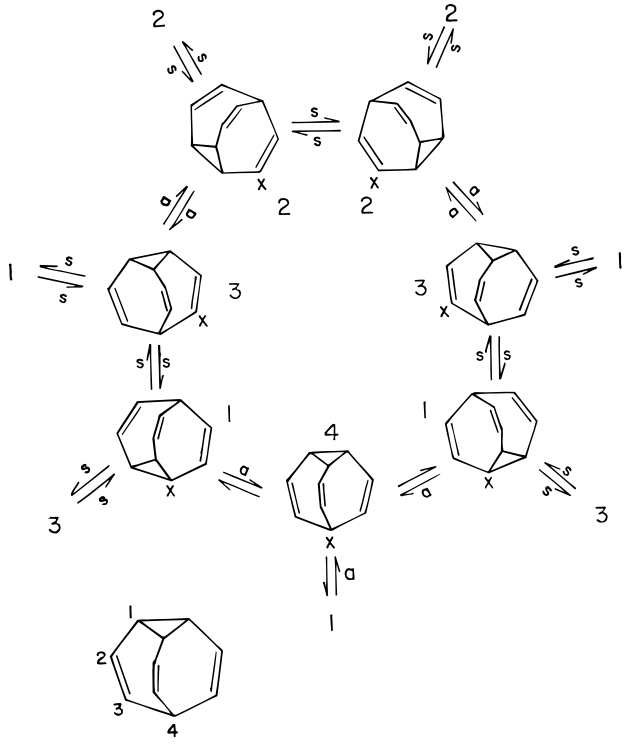

Figure 1. The isomerization cycle of monosubstituted bullvalenes. The substituent is labeled by X and the isomers are labeled according to the substitution site (see insert at the bottom left part of the figure). The letters *a* or *s* indicate whether the interconversion involves cleavage of a cyclopropane-ring bond which lies opposite or adjacent to the substituted wing, respectively. There are two equivalent *s*-type reactions leading to the same isomer, one inside the cycle and one outside, leading to further branching of the permutation scheme.

possible isomers labeled 1, 2, 3, or 4 depending on the substitution site. Their interconversion can be expressed in terms of the cycle of seven Cope rearrangement steps shown in Figure 1.[2,16,17] Thus isomer 4 (see insert in Figure 1 for the labeling system used) can only interconvert to isomer 1 by cleavage of one of the cyclopropane-ring bonds. There are three equivalent pathways, two of which are shown within the cycle, one more points out of the cycle. Isomer 1 can revert to 4 by cleavage of the cyclopropane bond opposite the wing carrying the substituent (labeled *a* for anti) or interconvert to 3 by cleavage of one of the bonds adjacent to the substituted wing (labeled *s* for syn). The second *s*-cleavage also leads to isomer 3 as indicated by the outgoing arrow. Similarly, 3 can revert to 1 by *s*-cleavage or interconvert to 2 by *a*-cleavage. The latter can either revert to 3 by an *a*-cleavage or interconvert to a degenerated form of isomer 2 by *s*-cleavage, etc. The important point to notice is that the Cope rearrangement allows only certain specific transformations; direct interconversion of, for example, 4 and 3 or 1 and 2 are not allowed. In solution the two *s*-cleavages are equally probable, but in general they have a different probability than an *a*-cleavage. These considerations must be taken into account when analyzing the dynamic NMR spectra discussed below.

Experimental Section

The substituted bullvalenes were kindly provided by Professor G. Schröder from the University of Karlsruhe.

Carbon-13 and proton high resolution NMR spectra were recorded on a Bruker AM500 spectrometer (11.74 T). Fluorine-19 spectra were measured on a Bruker AMX400 spectrometer (9.4 T). Most measurements on fluoro- and cyanobullvalene were performed in deuterated methylene chloride solutions, some were made in $CDCl_3$, and for higher temperatures deuterated dimethyl sulfoxide (DMSO) was used. Bullvalenecarboxylic acid was measured in 1:1 mixtures of CD_2Cl_2/CD_3OD.

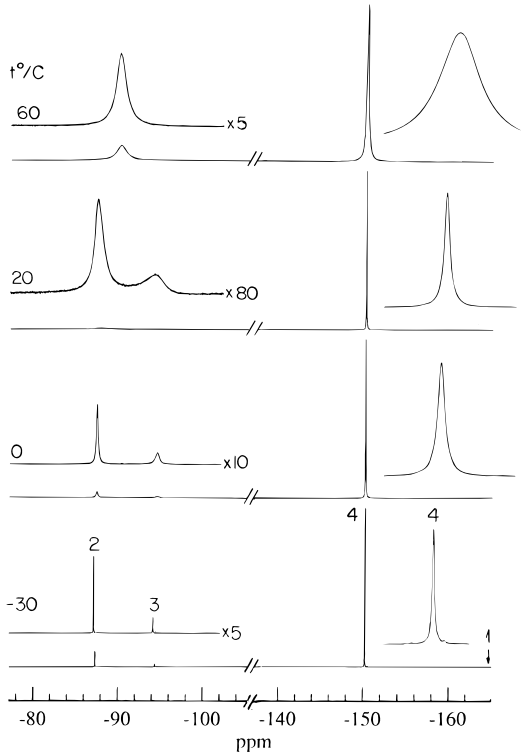

Figure 2. Proton decoupled fluorine-19 NMR spectra of a 3 wt % solution of fluorobullvalene in CD_2Cl_2 (bottom three traces) and in $CDCl_3$ (top trace) at the indicated temperatures. The ppm scale is relative to $CFCl_3$ (taking $\delta(C_6F_6) = -163$ ppm). The arrow at −165.35 ppm indicates the chemical shift of isomer 1. The signals of isomers 2 and 3 are inserted at higher gain, as indicated on the same chemical shift scale. The signal of isomer 4 is also inserted but on a chemical shift scale expanded by ×22.2 relative to that given in the bottom, in order to emphasize the shift and nonmonotonic broadening of the line, at the first onset of broadening. The ^{19}F $\pi/2$ pulse width was 15 μs, and the proton decoupling field strength corresponded to 2.5 kHz.

Results and Discussion

A. Fluorobullvalene. The rearrangement processes of fluorobullvalene in solution were studied many years ago by Oth et al.,[3] using proton and fluorine NMR. They found that this compound exists in solutions, predominantly as isomer 4 at equilibrium with small amounts of isomers 2 and 3. Since the interconversion between these species must involve isomer 1, they concluded that the latter also exists in the solution but at quantities too small to detect directly by NMR. We have reinvestigated this system using fluorine-19 and carbon-13 NMR, confirming the earlier conclusions of Oth et al. and deriving accurate values for the equilibrium concentrations of the various isomers and the kinetic parameters for their interconversion rate constants.

A1. ^{19}F NMR. Proton decoupled ^{19}F NMR spectra of a 3 wt % solution of fluorobullvalene in deuterated methylene chloride are shown in Figure 2. At −30 °C three peaks are observed at −150.05, −94.26, and −87.33 ppm with relative intensities of 0.870, 0.096, and 0.034. We identify these peaks with those due to isomers 4, 2, and 3, respectively. This assignment is based on the relative abundance of the isomers, as determined from the carbon-13 spectra, to be described below.

(16) Klose, H.; Günther, H. *Chem. Ber.* **1969**, *102*, 2230.
(17) Paquette, L. A.; Malpass, J. R.; Krow, G. R.; Barton, T. J. *J. Am. Chem. Soc.* **1969**, *91*, 5296.

Scheme 1

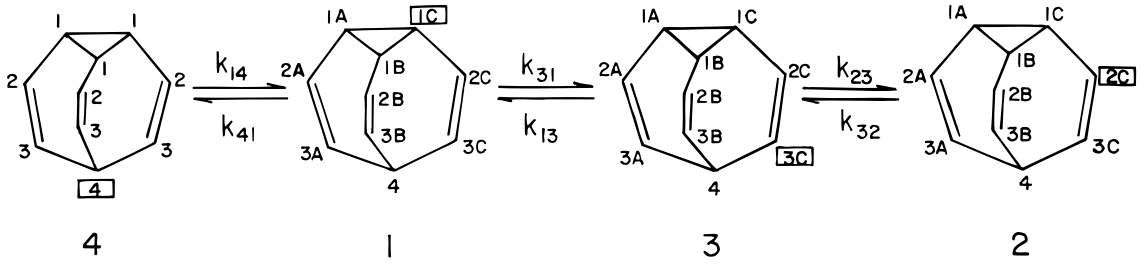

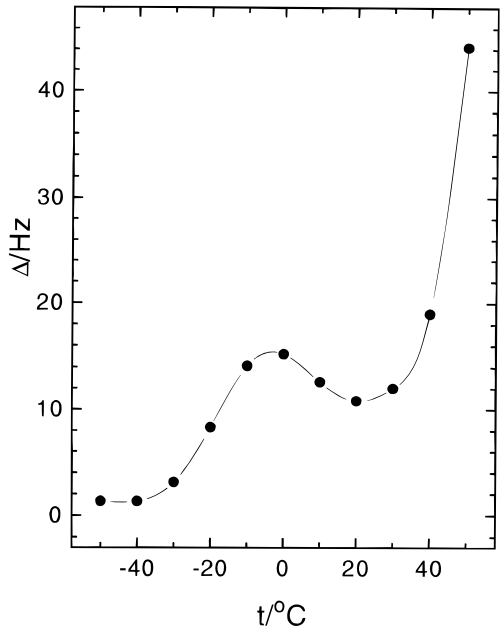

Figure 3. The line width (at half maximum height) of the fluorine-19 NMR signal, due to isomer 4, of fluorobullvalene in the same solution as used for Figure 2, as a function of temperature.

As the temperature is raised, a gradual line broadening sets in due to interconversion between the various isomers. Close examination of the spectra shows that the first peak to broaden is that of isomer 4, but its broadening is not monotonic with increasing temperature. The peak first broadens up to a maximum value of ~15 Hz (full width at half maximum intensity), and then it narrows slightly, followed by a sharp increase in the line width. At the same time there is a small but distinct shift of the line to high field (see inserts in Figure 2). A plot of the line width of isomer 4 as a function of temperature is shown in Figure 3. Within the framework of the Cope rearrangement cycle of Figure 1, this nonmonotonic line broadening can only be explained in terms of interconversion between the dominant signal of isomer 4 with a very weak (unobservable) signal of isomer 1. Under such conditions, the line width of the dominant signal (4) is given by[18]

$$\Delta\frac{1}{T_2(4)} = \frac{1}{T_2(4)} - \frac{1}{T_2^0(4)} = P_1\frac{(\omega_1-\omega_4)^2 k_{41}}{k_{41}^2+(\omega_1-\omega_4)^2} \qquad (1)$$

where ω_i is the chemical shift of species i (in rad s^{-1}), k_{ij} is the rate constant for the transformation of isomer j to isomer i, and P_i is the fractional population of isomer i, and we assumed that $P_1 \ll P_4 \approx 1$. The maximum of $\Delta(1/T_2(4))$ occurs when $k_{41} \approx |\omega_1 - \omega_4|$ and its value is[18]

$$\Delta\frac{1}{T_2(4)}(\max) = \frac{1}{2}P_1|\omega_1-\omega_4| \qquad (2)$$

These relations give information on the product of P_1 and $|\omega_1 - \omega_4|$, both of which are unknown, although from the upfield shift of line 4 with temperature we can deduce the $\delta_1 < \delta_4$ (algebraically). We have recorded a low temperature (−55 °C) fluorine-19 spectrum of fluorobullvalene under conditions of excessive averaging and in fact observed a very small peak at −165.35 with about 0.2% intensity relative to that of line 4. Upon heating to above −40 °C it immediately broadened beyond detection. For the rest of the analysis we therefore identify this peak with the fluorine resonance of isomer 1. Its relative intensity at −3 °C (where the line width of the peak due to isomer 4 passes through a local maximum (see (Figure 3)) was determined by eq 2, using the now known $(\omega_1 - \omega_4)$ value. For the rest of the temperature range, P_1 was determined together with the relevant rate constants by best fitting the overall results with simulated dynamic spectra. These spectra were calculated from the general time domain solution of the Bloch−McConnell equations for the transverse magnetization, $\bar{M}(t)$ of the interchanging spins

$$\bar{M}(t) = C\{\exp[K-(R+i\Omega)]t\}\bar{P} \qquad (3)$$

Here C is a constant (which depends on the concentration of the solution, the temperature and certain physical constant), $\bar{P}$ is a column vector comprising the fractional populations P_i of the interchanging isomers, R and Ω are diagonal matrices with elements, $1/T_2^0(i)$ and ω_i, respectively, and K is the exchange matrix. For the ^{19}F spectra K is given by the following 4 × 4 matrix

$$K = \begin{vmatrix} -k_{14} & k_{41} & & \\ k_{14} & -k_{41}-k_{31} & k_{13} & \\ & k_{31} & -k_{13}-k_{23} & k_{32} \\ & & k_{23} & -k_{32} \end{vmatrix} \qquad (4)$$

where k_{ij} is the rate constant for the interconversion of species j to i, as indicated in Scheme 1 with $k_{ij}/k_{ji} = P_i/P_j$. This scheme also shows the labeling system used in this paper. For each isomer the substituted carbon is enclosed in a square. The rate constants, k_{ij}, and the fractional populations, P_i, were first estimated using approximate equations for the slow exchange regime and from the relative peak intensities, in this limit. This was followed by best fitting the whole spectra to eq 3. The final results are summarized in Figure 4. They include a global fit to the ^{19}F as well as the ^{13}C experiments, described in the next section. A summary of the magnetic, kinetic, and thermodynamic parameters derived from these results is given in Tables 1 and 2.

A2. Carbon-13 NMR. Additional kinetic information and confirmation of the ^{19}F results were obtained from natural abundance ^{13}C spectra of the fluorobullvalene solutions. The spectrum of a 3 wt % solution in deuterated methylene chloride at −55 °C is shown in Figure 5. The labeling of the peaks is as in the diagram above with the superscript indicating the isomer. The spectrum consists of three sets of lines, with approximate intensities, 1.0; 0.065; 0.018. The weaker sets are

(18) Sandström, J. Dynamic NMR Spectroscopy; Academic Press: London, 1982; Chapter 6.

Table 1. ^{13}C Chemical Shifts (Relative to TMS) and Spin−Spin Coupling Constants (Absolute Values) for the Various Isomers of Fluorobullvalene, Measured in CD_2Cl_2 at −55 °C

	isomer 1	isomer 2			isomer 3			isomer 4		
	δ_i (ppm)	δ_i (ppm)	J_{C_i-F} (Hz)	$^1J_{C_i-H}$ (Hz)	δ_i (ppm)	J_{C_i-F} (Hz)	$^1J_{C_i-H}$ (Hz)	δ_i (ppm)	J_{C_i-F} (Hz)	$^1J_{C_i-H}$ (Hz)
1AB	21.26	18.54		166.6	19.07		(a)			
								20.10		169.0
1C	(70)[b]	22.43	40.3	166.4	19.35	9.2	(a)			
2AB	125.60	126.15		158.8	128.22		160			
								123.80	15.8	160.8
2C	(123)[b]	155.17	246.6		101.12	21.1	(a)			
3AB	127.08	127.91		164.9	124.47		157.9			
								131.61	35.7	166.1
3C	(125)[b]	101.60	13.4	162.8	158.40	270.1				
4	31.9	26.63	10.1	133.8	34.04	29.9	134	91.11	161.4	

[a] Not determined. [b] Estimated values used in the simulation.

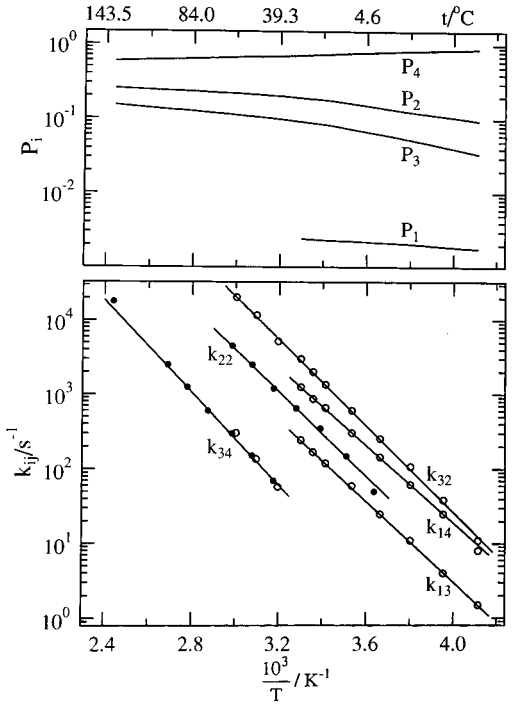

Figure 4. Semilogarithmic plots of the fractional populations of the four fluorobullvalene isomers (top) and of the various interconversion rate constants, k_{ij} (bottom) as function of the reciprocal absolute temperature, obtained from the fitting of the ^{19}F and ^{13}C spectra in the various solutions. Open circles are experimental results obtained from ^{19}F spectra, closed circles from ^{13}C spectra.

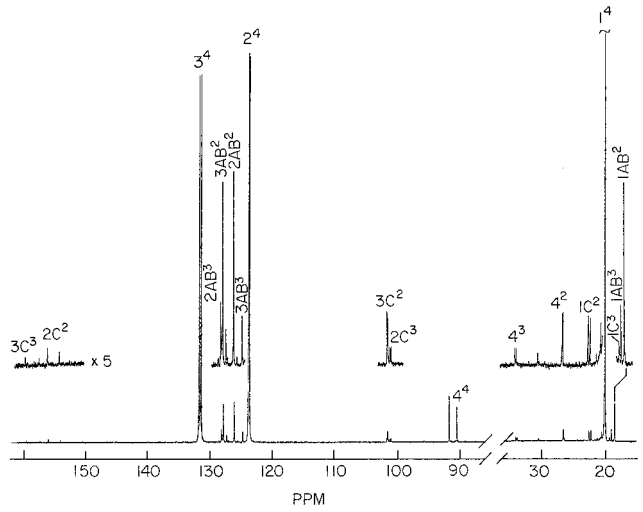

Figure 5. A proton decoupled carbon-13 NMR spectrum of a 3 wt % solution of fluorobullvalene in CD_2Cl_2 at −55 °C. Regions in the spectrum with weak peaks are inserted at a five-fold gain. The peak assignments are explained in the text. Note the doubling of some of the peaks due to spin−spin coupling with the ^{19}F nuclei. Sixty degree carbon-13 pulses of 4 μs width were used with a proton decoupling field strength corresponding to a 3.6 kHz.

replotted at a five-fold gain on the same chemical shift scale. The strong peaks in the spectrum are readily identified with isomer 4. Note that except for carbon 1^4 all signals of this isomer are doublets, due to spin−spin coupling with the fluorine nucleus. Peak 4^4 is considerably weaker than expected stoichiometrically, apparently due to the weaker NOE experienced by the bridgehead carbon atom. The weaker peaks in the carbon-13 spectrum are due to isomers 2 and 3. An unambiguous assignment of these peaks could be made on the basis of the proton spectrum, the carbon-13 (proton undecoupled) spectrum, two dimension $^{13}C-^1H$ correlation, carbon-13 2D-exchange spectroscopy and best fit to the dynamic 1D spectra. A summary of the magnetic parameters so obtained is given in Table 1.

When all peaks of isomers 2, 3, and 4 were identified, a number of extremely weak unassigned peaks still remained. Four of these (at 20.63, 30.52, 127.37, and 128.11 ppm) were ascribed to unsubstituted bullvalene, while similarly weak peaks (of the order of 10^{-3} relative to those of isomer 4) were ascribed to isomer 1. As in the case of the ^{19}F resonance its presence in the solution was confirmed by the behavior of the dynamic spectra. The chemical shift values of isomer 1 used in the simulation of the dynamic spectra are included in Table 1. Some of these assignments must, however, be considered as tentative.

In Figure 6 are shown ^{13}C spectra of the same solution as in Figure 5 but recorded at higher temperatures, up to 32 °C, as well as a spectrum in a DMSO solution (3 wt %) at 87 °C. It may be seen that the peaks undergo typical line broadening as expected from the effect of dynamic processes. Some of the lines due to isomer 4 exhibit a nonmonotonous behavior: broadening, followed by narrowing, and then broadening again, similar to that observed for the ^{19}F spectrum of this isomer. We have performed a complete quantitative kinetic analysis of such temperature dependent spectra, including in particular, best fitting of the line shapes due to the less abundant isomers 2 and 3. The peaks due to these isomers are sensitive to the same rearrangement processes already discussed in connection with the ^{19}F spectra and in addition also to k_{22}, the rate constant for the degenerate interconversion of isomer 2 (top part of Figure 1). When the appropriate statistics are considered, the exchange matrix for the carbon-13 spectrum acquires the form shown in Table 3. For the simulation of the ^{13}C spectra two subspectra were superposed corresponding, respectively, to the molecules with the ^{19}F in the α and β states and assuming that all the $^1J_{C-F}$'s have the same sign. The results for both the ^{19}F and ^{13}C spectra became insensitive to isomer 1 above room

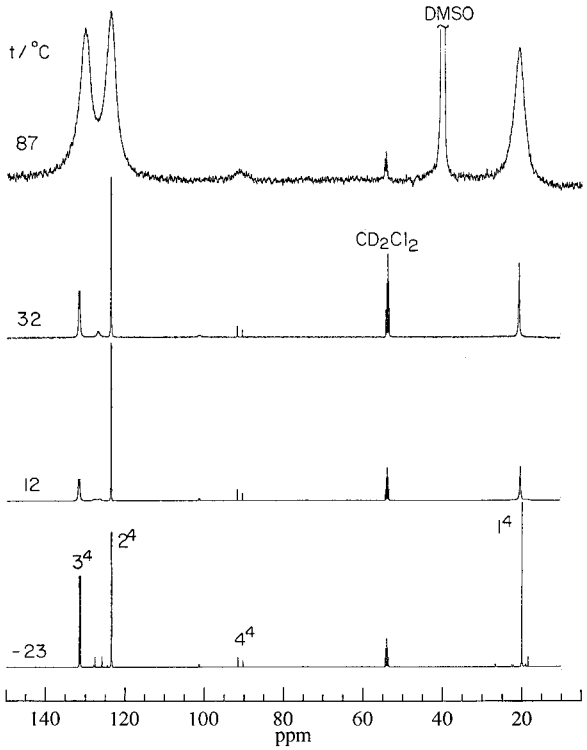

Figure 6. Proton decoupled carbon-13 spectra of fluorobullvalene solutions as function of temperature. The bottom three spectra are for the same solution as in Figure 5. The top trace is for a 3 wt % solution in DMSO. Only the lines due to the dominant isomer 4 are indicated. Experimental conditions are as in Figure 5.

Table 2. Summary of Kinetic and Thermodynamic Parameters for the Various Fluorobullvalene Isomers

A. Kinetic Parameters, $k_{ij} = A\exp(-E_a/RT) = (k_BT/h)\exp(-\Delta G^{\ddagger}/RT)$

	A ($\times 10^{-11}$) (s^{-1})	E_a (kcal mol^{-1})	$\Delta G^{\ddagger}$ (300 K) (kcal mol^{-1})	$\Delta S^{\ddagger}$ (eu)
k_{14}	4.4	11.9	13.5	−7.3
k_{13}	2.2	12.4	14.4	−8.7
k_{32}	102.5	13.3	13.0	−1.0
k_{22}	12.1	13.0	13.9	−5.3
k_{34}	5.2	14.2	15.7	−6.9

B. Thermodynamic Parameters, $K = [B]/[A] = \exp(-\Delta G/RT) = \exp(-\Delta H/RT)\exp(\Delta S/R)$

[B]/[A]	ΔG (300 K) (kcal mol^{-1})	ΔH (kcal mol^{-1})	ΔS (eu)
[1]/[4]	3.41	1.26	−7.2
[3]/[1]	−2.21	1.78	13.3
[2]/[3]	−0.46	−0.52	−0.21

temperature. At higher temperatures we therefore suppressed isomer 1 and used contracted exchange matrices. Equation 4 for the fluorine spectrum then becomes

$$K = \begin{pmatrix} -k_{34} & k_{43} & \\ k_{34} & -k_{43} - k_{23} & k_{32} \\ & k_{23} & -k_{32} \end{pmatrix} \qquad (5)$$

while instead of the exchange matrix in Table 3, the one shown in Table 4 was used. In these matrices k_{34} are the direct interconversion rate constants between isomers 4 and 3. It is related to the k_{ij}'s involving isomer 1 by the relation

$$k_{34} = k_{14}\frac{k_{31}}{k_{41} + k_{31}} \qquad (6)$$

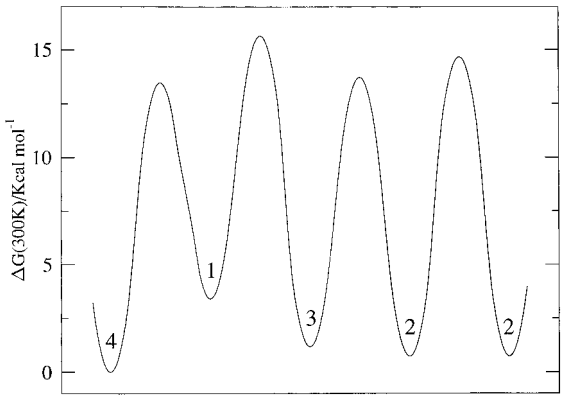

Figure 7. A schematic free energy diagram (at 300 K) relating the ground and transition states of the various fluorobullvalene isomers. The vertical scale is calculated from the thermodynamic and kinetic parameters of Table 2, taking isomer 4 as reference.

Within our experimental accuracy we have not detected any solvent effect on the k_{ij}'s and the K's on going from the low temperature solvents (CD_2Cl_2, $CDCl_3$) to that used at higher temperatures (DMSO).

A final comment concerning the fitting procedure relates to the nonstoichiometric peak intensities, in particular those of the fluorine bonded carbons, due to differences in the NOE efficiency. The situation is similar to that as in a nonequilibrium system[19] and was accounted for in the simulation by substituting the vector $\bar{P}$ in eq 3 by the vector $\bar{I}$ whose components are proportional to the observed peak intensities (at low temperatures) rather than to their expected stoichiometric intensities.

The overall results of Figure 4 and of Table 2 can also be expressed in terms of a free energy potential diagram. Using Eyring's absolute rate theory, we write the free energy of the transition states involved in the $j \rightarrow i$ transformation by

$$k_{ij} = \kappa\frac{k_BT}{h}e^{-\Delta G^{\ddagger}/RT} = \kappa\frac{k_BT}{h}e^{-\Delta H^{\ddagger}/RT}e^{\Delta S^{\ddagger}/R} \qquad (7)$$

where we took the transmission coefficient, κ, as unity. Using the ΔG and $\Delta G^{\ddagger}$ values calculated from the equilibrium and rate constants of Figure 4 the potential free energy diagram (at 300 K) shown in Figure 7 is obtained. It shows quantitatively the relations between the various ground and transition states involved in the tautomeric cycle of Figure 1.

B. Cyanobullvalene. The ^{13}C NMR spectrum of cyanobullvalene in solution was studied earlier by Zwez.[20] He identified two isomers of this compound with the dominant one being isomer 3 and the minor being isomer 2. At low temperatures well resolved NMR spectra of both isomers are observed, while on heating to above −30 °C, line broadening due to the Cope rearrangement sets in. As for fluorobullvalene a complete interpretation of these dynamic spectra is quite complicated and must involve isomers whose concentrations are too low to observe.

B1. The Low Temperature ^1H and ^{13}C NMR Spectra. A proton 500 MHz NMR spectrum of cyanobullvalene in CD_2Cl_2 at −30 °C, with its peak assignment, is shown in the upper trace of Figure 8. Only the strong peaks due to isomer 3 are identified. Those due to isomer 2 were too weak and too close to the peaks of isomer 3 for an unequivocal identification. The assignment of the isomer 3 peaks is based on multiple $^1H-^1H$

(19) Ernst, R. R.; Bodenhousen, G.; Wokaun, A. Principles of Nuclear Magnetic Resonance in One and Two Dimensions; Clarendon Press: Oxford, 1987; p 209.

(20) Zwez, T. Ph.D. Dissertation, Karlsruhe University, 1988.

Table 3. The Full Exchange Matrix for the Carbon-13 Nuclei in the Four Isomers of Fluorobullvalene

	1^4	2^4	3^4	$1AB^1$	$2AB^1$	$3AB^1$	$2C^1$	$3C^1$	4^1	$1AB^3$	$2AB^3$	$3AB^3$
1^4	$-k_{14}$					k_{41}			k_{41}			
2^4		$-k_{14}$			k_{41}			k_{41}				
3^4			$-k_{14}$	k_{41}			k_{41}					
$1AB^1$			$\frac{2}{3}k_{14}$	$-k_{41}-k_{31}$								$\frac{1}{2}k_{13}$
$2AB^1$		$\frac{2}{3}k_{14}$			$-k_{41}-k_{31}$						$\frac{1}{2}k_{13}$	$\frac{1}{2}k_{13}$
$3AB^1$	$\frac{2}{3}k_{14}$					$-k_{41}-k_{31}$				$\frac{1}{2}k_{13}$	$\frac{1}{2}k_{13}$	
$2C^1$			$\frac{1}{3}k_{14}$				$-k_{41}-k_{31}$					
$3C^1$		$\frac{1}{3}k_{14}$						$-k_{41}-k_{31}$				
4^1	$\frac{1}{3}k_{14}$								$-k_{41}-k_{31}$	$\frac{1}{2}k_{13}$		
$1AB^3$						$\frac{1}{2}k_{31}$			k_{31}	$-k_{13}-k_{23}$		
$2AB^3$					$\frac{1}{2}k_{31}$	$\frac{1}{2}k_{31}$					$-k_{13}-k_{23}$	
$3AB^3$				$\frac{1}{2}k_{31}$	$\frac{1}{2}k_{31}$							$-k_{13}-k_{23}$
$1C^3$								k_{31}				
$2C^3$							k_{31}					
4^3				$\frac{1}{2}k_{31}$								
$1AB^2$												k_{23}
$2AB^2$											k_{23}	
$3AB^2$										k_{23}		
$1C^2$												
$3C^2$												
4^2												
4^4												
$1C^1$												
$3C^3$												
$2C^2$												

homonuclear decoupling experiments. The resulting chemical shifts and spin−spin coupling constants are summarized in Table 5A.

A ^{13}C NMR spectrum of the same solution as above, at −40 °C, is shown in the bottom trace of Figure 9. The spectrum exhibits two sets of lines at a ratio of ∼13:1, corresponding, respectively, to isomers 3 and 2. The assignment shown in the figure is based on $^1H-^{13}C$ correlation and 2D exchange spectroscopy. The chemical shifts and $^1J_{C-H}$'s, derived from these spectra, are summarized in Table 5B. The results are consistent with those of Zwez.[20]

B2. The Carbon-13 Dynamic Spectra of Cyanobullvalene. On heating the solution of cyanobullvalene to above −30 °C all lines in the spectrum gradually broadened (see examples of spectra in Figure 9). However, while the peaks due to the cyano carbons (CN^3 and CN^2) and the carbons directly attached to the cyano group ($3C^3$ and $2C^2$) rapidly coallesce (pairwise), the other peaks broadened and eventually converge with the base line noise (see top spectrum at 123 °C in DMSO-d_6). Qualitatively, this behavior reflects the interconversion of isomers 3 and 2.

$$\text{isomer 3} \underset{k_{32}}{\overset{k_{23}}{\rightleftharpoons}} \text{isomer 2}$$

However, this process alone cannot account quantitatively for the observed evolution of the spectrum. Inspection of Table 3 shows that this mechanism alone leads to pairwise coalescence of groups of carbon signals, for example, $1AB^3$ and $3AB^2$; $1C^3$ and 4^2; in addition to the pairs CN^3 and CN^2; $3C^3$ and $2C^2$, contrary to observation. Thus, although the interconversion of isomers 3 and 2 certainly takes place, as we have in fact confirmed by 2D exchange spectroscopy, additional mechanisms must be considered.

To proceed it is natural to invoke the degenerate interconversion of isomer 2

$$\text{isomer 2} \underset{k_{22}}{\overset{k_{22}}{\rightleftharpoons}} \text{isomer 2}$$

When this is included in the simulation, all lines, except those

Table 3 (Continued)

$1C^3$	$2C^3$	4^3	$1AB^2$	$2AB^2$	$3AB^2$	$1C^2$	$3C^2$	4^2	4^4	$1C^1$	$3C^3$	$2C^2$
		k_{13}										
	k_{13}											
k_{13}												
					k_{32}							
				k_{32}								
			k_{32}									
$-k_{13}-k_{23}$								k_{32}				
	$-k_{13}-k_{23}$						k_{32}					
		$-k_{13}-k_{23}$				k_{32}						
			$-k_{32}-k_{22}$		$\frac{1}{2}k_{22}$			k_{22}				
				$-k_{32}-\frac{1}{2}k_{22}$	$\frac{1}{2}k_{22}$							
			$\frac{1}{2}k_{22}$	$\frac{1}{2}k_{22}$	$-k_{32}-k_{22}$							
		k_{23}				$-k_{32}-k_{22}$	k_{22}					
	k_{23}					k_{22}	$-k_{32}-k_{22}$					
k_{23}			$\frac{1}{2}k_{22}$					$-k_{32}-k_{22}$				
									$-k_{14}$	k_{41}		
									k_{14}	$-k_{41}-k_{31}$	k_{13}	
										k_{31}	$-k_{13}-k_{23}$	k_{32}
											k_{23}	$-k_{32}$

associated with the group $C - CN$ indeed coalesce (see the entries k_{22} in Table 3). However, as it turned out, this addition was still not sufficient for quantitatively reproducing the experimental line width. Additional species, not observed in the NMR spectrum, in particular isomer 1 and possibly also isomer 4, must be assumed to be present in the solution and participate in the rearrangement process. This can readily be seen by the following considerations. In Figure 10 are plotted the (full) line width (at half maximum intensity) of the observed peaks in the temperature region −50 °C to +20 °C. The curves labeled $3C^3$ and CN^3 correspond to the indicated carbons below their coalescence temperatures and to the combined $3C^3/2C^2$ and CN^3/CN^2 signals above these temperatures. The widths of these peaks are independent of k_{22}, while the rearrangement (3) ⇄ (2) alone should result in broadening, coalescence, and narrowing behavior given by an equation similar to eq 1, with the indices 1,4 substituted by 2,3. The expected maximum broadening is then given by

$$\Delta\frac{1}{T_2(3)}(\max) = \frac{1}{2}P_2|\omega_2 - \omega_3| \qquad (8)$$

From Table 5B, $|\omega_2 - \omega_3|$ is 253 and 166 s^{-1} for the $2C^2$, $3C^3$ and CN^2, CN^3 pairs, which, with $P_2 = 0.05$ leads to a calculated maximum broadening of ∼2.0 and 1.3 Hz, respectively. While for CN^3 the experimental maximum broadening indeed does not exceed a few Hz, for $3C^3$ it is almost 40 Hz, far more than the expected 2 Hz. The only way such an extra broadening can be induced is via exchange with an additional species, which although may be too weak to observe, has a very large chemical shift to cause the observed broadening. The only species that can cause this effect is isomer 1 and perhaps also isomer 4. A quantitative analysis of the line shape would require the knowledge of the concentration and chemical shifts of these species. In the absence of this information we will limit ourselves to a semiqualitative analysis.

Table 4. A Contracted Exchange Matrix as in Table 3 with Isomer 1 Taken as a Transient Species

	1^4	2^4	3^4	$1AB^3$	$2AB^3$	$3AB^3$	$1C^3$	$2C^3$	4^3	$1AB^2$	$2AB^2$	$3AB^2$	$1C^2$	$3C^2$	4^2	4^4	$3C^3$	$2C^2$
1^4	$-k_{34}$			k_{43}	$\frac{1}{2}k_{43}$													
2^4		$-k_{34}$			$\frac{1}{2}k_{43}$	$\frac{1}{2}k_{43}$	k_{43}											
3^4			$-k_{34}$			$\frac{1}{2}k_{43}$		k_{43}	k_{43}									
$1AB^3$	$\frac{2}{3}k_{34}$			$-k_{43}-k_{23}$								k_{32}						
$2AB^3$	$\frac{1}{3}k_{34}$	$\frac{1}{3}k_{34}$			$-k_{43}-k_{23}$						k_{32}							
$3AB^3$		$\frac{1}{3}k_{34}$	$\frac{1}{3}k_{34}$			$-k_{43}-k_{23}$				k_{32}								
$1C^3$		$\frac{1}{3}k_{34}$					$-k_{43}-k_{23}$								k_{32}			
$2C^3$			$\frac{1}{3}k_{34}$					$-k_{43}-k_{23}$						k_{32}				
4^3			$\frac{1}{3}k_{34}$						$-k_{43}-k_{23}$				k_{32}					
$1AB^2$						k_{23}				$-k_{32}-k_{22}$		$\frac{1}{2}k_{22}$			k_{22}			
$2AB^2$					k_{23}						$-k_{32}-\frac{1}{2}k_{22}$	$\frac{1}{2}k_{22}$						
$3AB^2$				k_{23}						$\frac{1}{2}k_{22}$	$\frac{1}{2}k_{22}$	$-k_{32}-k_{22}$						
$1C^2$									k_{23}				$-k_{32}-k_{22}$	k_{22}				
$3C^2$								k_{23}					k_{22}	$-k_{32}-k_{22}$				
4^2							k_{23}			$\frac{1}{2}k_{22}$					$-k_{32}-k_{22}$			
4^4																$-k_{34}$	k_{43}	
$3C^3$																k_{34}	$-k_{43}-k_{23}$	k_{32}
$2C^2$																	k_{23}	$-k_{32}$

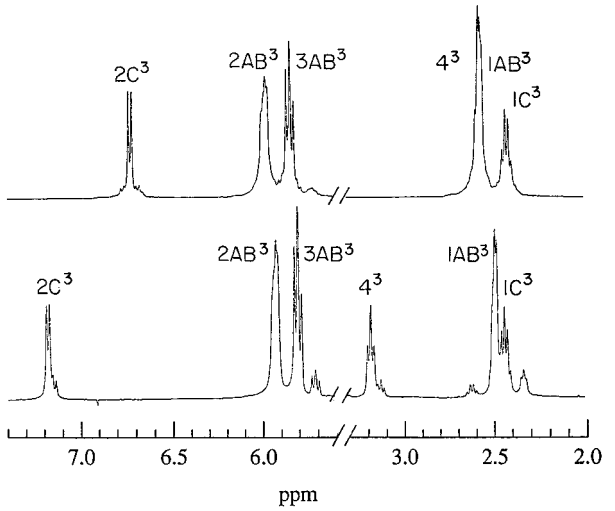

Figure 8. Top: Proton NMR spectra of a 3 wt % solution of cyanobullvalene in CD_2Cl_2 at −30 °C. Bottom: a 1.5 wt % solution of bullvalenecarboxylic acid in a 1:1 mixture of CD_3OD/CD_2Cl_2 at −38 °C. Only the peaks due to the dominant isomer 3 are assigned. Fifty degree pulses of 6 μs width were used.

Table 5. ^{1}H and ^{13}C Magnetic Parameters for Cyanobullvalene (in CD_2Cl_2 at −30 °C) and Bullvalenecarboxylic Acid (in 1:1 CD_2Cl_2/CD_3OD Mixture at −38 °C)

A. Proton Chemical Shifts and Spin−Spin Coupling Constants for Isomers 3

	δ_i, (ppm)			$^3J_{ij}$, (Hz)	
H-atom	CN	COOH	H−H pair	CN	COOH
1AB	2.56	2.48	1AB − 1C	8.4	8.1
1C	2.41	2.43	1AB − 2AB		
2AB	5.97	5.92	2AB − 3AB	11.3	10.8
2C	6.72	7.17	3AB − 4	8.3	8.7
3AB	5.83	5.80	1C − 2C	8.4	8.0
4	2.57	3.17			

B. Carbon-13 Chemical Shifts and $^1J_{C-H}$ Spin−Spin Coupling Constants for Isomers 3 and 2

	cyanobullvalene				bullvalenecarboxylic acid			
	isomer 3		isomer 2		isomer 3		isomer 2	
	δ_i, (ppm)	$^1J_{C^i-H}$	δ_i, (ppm)	$^1J_{C^i-H}$	δ_i, (ppm)	$^1J_{C^i-H}$, (Hz)	δ_i, (ppm)	$^1J_{C^i-H}$, (Hz)
1AB	23.43	169	19.76	166	23.17	167	19.97	167
1C	21.50	171	22.33	160	21.68	169	18.66	170
2AB	128.69	161	128.39	159	128.04[b]	163[b]	126.12[b]	159[b]
3AB	126.25	166	126.06	164	128.14[b]	160[b]	128.78[b]	156[b]
2C	144.62	161	111.56		140.08	160	129.92	
3C	111.24		143.56	168	130.47		137.82	159
4	32.74	134	30.56	136	29.27	134	30.93	135
X[a]	120.41		120.20		169.07		170.09	

[a] CN carbon for cyanobullvalene and COOH carbon for bullvalene carboxylic acid. [b] The assignment of 2AB and 3AB is tentative and may be reversed.

First, we may assume that at low temperatures ($\lesssim$ −10 °C) where peaks due to isomer 2 can still be discerned, their width is solely due to the (2) $\rightleftarrows$ (2) and (2) $\rightleftarrows$ (3) interconversion, involving the rate constants k_{22} and k_{23} (k_{32}). Under these conditions k_{32} can be estimated from the width of the $2C^2$ and CN^2 peaks before they coalesce

$$k_{32} \approx \frac{1}{T_2} - \frac{1}{T_2^0} \quad \text{(for the peaks } 2C^2, CN^2\text{)} \qquad (9)$$

while k_{22} can be obtained from the width of the other peaks of isomer 2, by subtracting the contribution of k_{32} (see filled-in symbols in Figure 10),

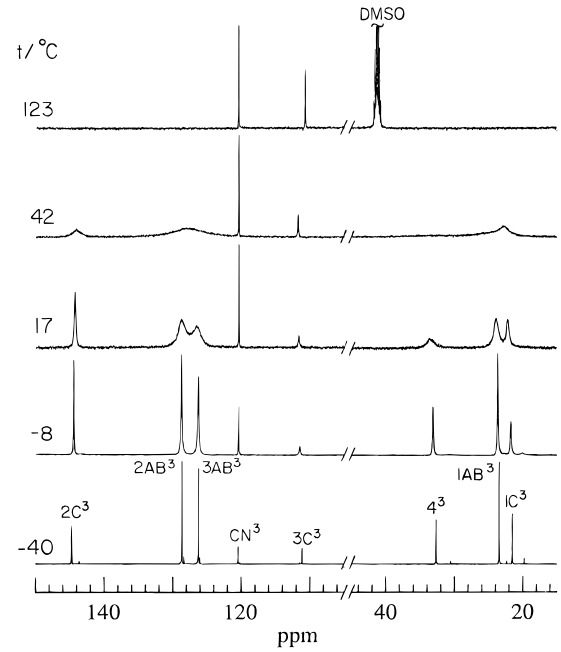

Figure 9. Proton decoupled carbon-13 NMR spectra of cyanobullvalene at different temperatures in the same solution as in Figure 8. Only signals due to the dominant isomer 3 are labeled. The weaker signals are due to isomer 2. Their assignment is included in Table 5B. Experimental conditions as in Figure 5.

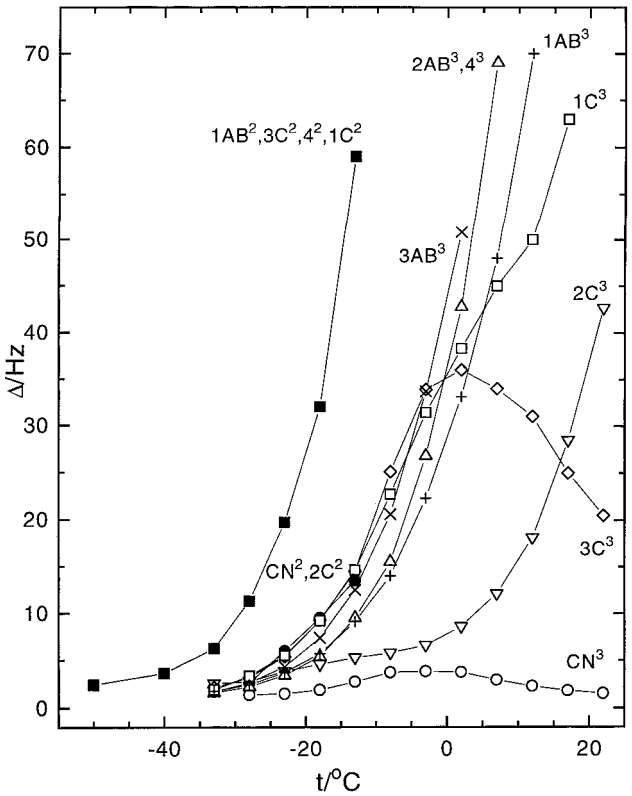

Figure 10. Full line widths at half maximum intensity of the ^{13}C peaks of isomer 2 (filled-in symbols) and isomer 3 (empty symbols) in a 3 wt % solution of cyanobullvalene in CD_2Cl_2 as function of temperature.

$$k_{22} \approx \frac{1}{T_2} - \frac{1}{T_2^0} - k_{32} \quad \text{(for peaks } 1AB^2, 3C^2, 4^2, 1C^2\text{)} \qquad (10)$$

Finally to estimate the rearrangement (3) $\rightleftarrows$ (1), we note that the broadening of the $3C^3$ peak, even before coalescence with $2C^2$ is more than expected from the rate of the (3) $\rightleftarrows$ (2) interconversion. If we assume that this extra broadening is due

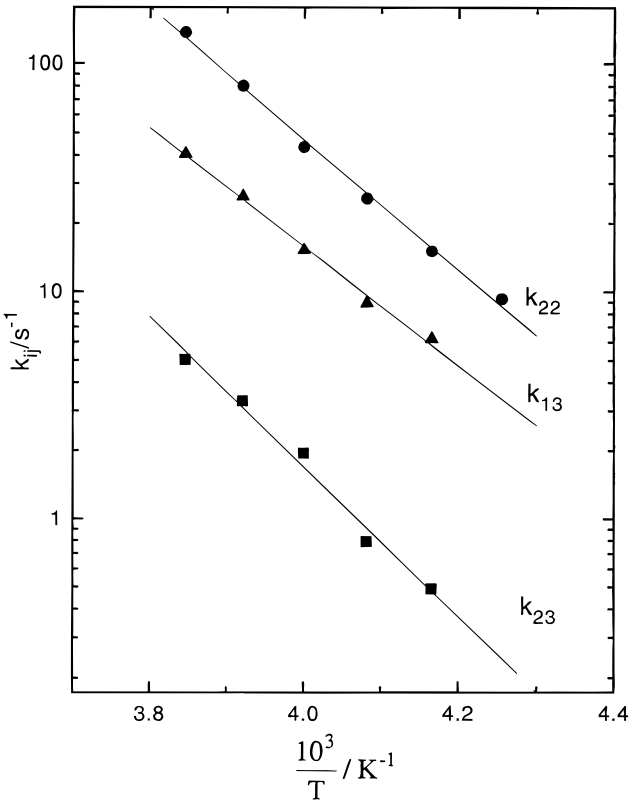

Figure 11. Arrhenius plots of various interconversion rate constants, k_{ij}, of the cyanobullvalene isomers, as estimated from the initial broadenings in Figure 10.

to exchange with the unobservable isomer 1 we can estimate k_{13} from

$$k_{13} = \frac{1}{T_2} - \frac{1}{T_2^0} - k_{23} \quad \text{(for peaks } 3C^3\text{)} \qquad (11)$$

The k_{ij}'s derived from eqs 9−11 (with $k_{23} = k_{32}$ (P_2/P_3) are plotted in Figure 11, and the corresponding kinetic parameters are summarized in Table 6.

It may be noted that some of the curves in Figure 10 exhibit a second step of broadening at around 20 °C (see the plots for $2C^3$ and $1C^3$). This is most likely due to the setting in of exchange with isomer 4 which can only be formed from isomer 1 (see (Figure 1). We have, however, not pursued the analysis further.

C. Bullvalenecarboxylic Acid. This compound behaves similar to cyanobullvalene. In solution it exists predominantly as isomer 3 and a small amount of isomer 2, with $P_2/P_3 \sim 0.17$ (at −38 °C). The proton NMR spectrum in CD_2Cl_2/CD_3OD at −38 °C is shown in the bottom part of Figure 8, and some ^{13}C spectra as a function of temperature are shown in Figure 12. The magnetic parameters derived from these spectra are included in Table 5. On heating, line broadening sets in with feature closely resembling those observed in cyanobullvalene. In particular the carbon signals of the C-COOH moiety coalesce pairwise and then remain sharp. Because of the lower solubility of bullvalenecarboxylic acid and hence the low signal intensity of the peaks due to isomer 2, no quantitative analysis was attempted in this case. Estimates of k_{23}, k_{22}, and k_{13} at −33 °C are, however, included in Table 6.

Summary

We have presented a detailed kinetic analysis of the dynamic high resolution solution spectra of fluorobullvalene and a semiquantitative analysis of cyanobullvalene and bullvalenecarboxylic acid. These monosubstituted bullvalenes can exist as four different isomers which interconvert via a thermally activated bond shift (Cope) rearrangement. In all cases signals due to more than one isomer were detected; three (and possibly four) in fluorobullvalene and two in the cyano and carboxylic acid derivatives. Yet, the analysis shows that essentially all four isomers are involved in the interconversion dynamics. Species, with concentrations too low to be detected by NMR, can still significantly affect the dynamic spectra if their chemical shifts are sufficiently large. A very detailed line shape analysis, preferably at different magnetic fields, may even provide good estimates for the equilibrium concentrations of such rare species. It is important to realize that these undetected isomers are not transition state species with life times of the order of bond vibrations. Such states would be too short-lived to affect the NMR frequencies and its line shape.

A comment about the accuracy of the results in Figures 4 and 11 and in Tables 2 and 6 is in order. These results are based on visual fitting of experimental and calculated spectra, and it is not straightforward to quantify the fit. In general the results for fluorobullvalene are considerably more accurate than for the two other compounds because the concentrations of three of the isomers could be directly determined from their peak intensity and a very good estimate of the concentration of the fourth isomer could be made. We estimate that the kinetic

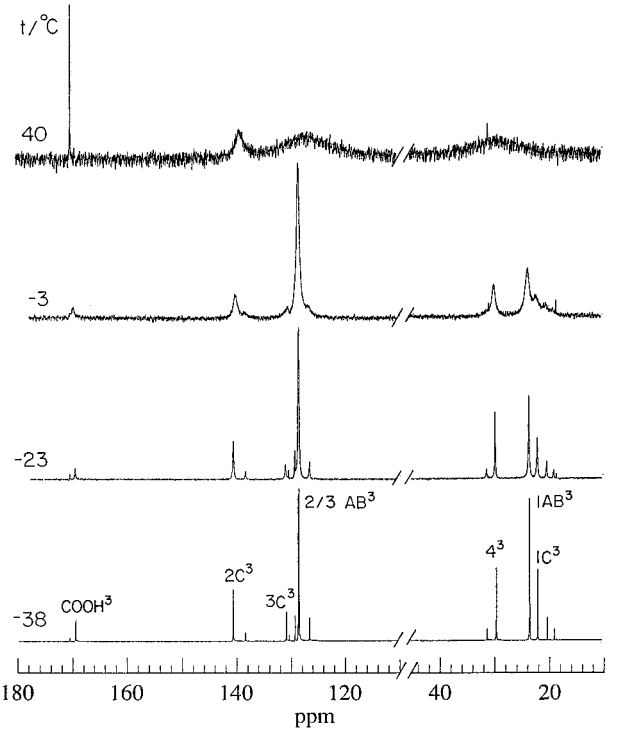

Figure 12. Proton decoupled carbon-13 NMR spectra of bullvalene carboxylic acid at different temperatures in the same solution as in the bottom part of Figure 8. Only signals due to isomer 3 are labeled. The weaker peaks are due to isomer 2. Their assignment is included in Table 5B. Experimental conditions are as in Figure 5.

Table 6. Kinetic Parameters for the Cope Rearrangement Processes in Cyanobullvalene and Bullvalenecarboxylic Acid

	cyanobullvalene		bullvalenecarboxylic acid
	k_{ij} (−33 °C) (s^{-1})	E_a (kcal mol^{-1})	k_{ij} (−33 °C) (s^{-1})
k_{23}	0.49	15.6	1.4
k_{22}	15.0	13.6	9.1
k_{13}	6.2	12.5	23.7

parameters in Table 2A are accurate to ±10%, while the fractional population for P_2 to P_4 in Figure 4 are better than ±5%; those for P_1 may however be off by as much as a factor 2. For the cyanobullvalene and bullvalenecarboxylic acid the rate constants involving the conversion of isomers 2 and 3 (k_{23} and k_{32}) and the interconversion of isomer 2 (k_{22}) are probably accurate to ±20% in the temperature range where they were directly determined (around −35 to −20 °C, see Table 6), but those involving isomer 1, k_{13}, are much less certain.

It is interesting to compare the kinetic parameters found for the Cope rearrangement in the monosubstituted bullvalenes with those found for the unsubstituted bullvalene. The latter was extensively studied by Oth et al.[2] for which they found $A \sim 2 \times 10^{13}$ s^{-1} and $E_a = 13.1$ kcal mol^{-1}. These results are similar to those for the interconversion rates between the dominant isomers in the monosubstituted bullvalenes studied here, i.e., isomers 2 and 3 of cyanobullvalene and bullvalenecarboxylic acid and isomer 4 of fluorobullvalene. Of course the reaction rates from the minor (unobserved) isomers to the more abundant ones are much higher. Thus, while the nature of the substituent is reflected in the distribution of the isomeric species in substituted bullvalenes, the energetics of the interconversion between different isomers in solution is very little affected by the substitution. As it turns out the situation in the solid state[14,15] is quite different.

Acknowledgment. We wish to dedicate this series of papers to Professor Gerhard Schröder on his recent retirement from his post as Professor of Chemistry in Karlsruhe University. Professor Schröder, who pioneered the field of bullvalene chemistry, supported us throughout our work on these interesting compounds and provided advice and materials for which we are most grateful. This research was supported by Grant No. 92-0094/5862 from the United States−Israel Binational Science Foundation (BSF), Jerusalem, Israel, and by the MINERVA Foundation, Munich, Germany.

JA954004T